



## Annular mode time scales in the Intergovernmental Panel on Climate Change Fourth Assessment Report models

E. P. Gerber,<sup>1,2</sup> L. M. Polvani,<sup>3</sup> and D. Ancukiewicz<sup>4</sup>

Received 15 August 2008; revised 26 September 2008; accepted 6 October 2008; published 27 November 2008.

[1] The ability of climate models in the Intergovernmental Panel on Climate Change Fourth Assessment Report to capture the temporal structure of the annular modes is evaluated. The vertical structure and annual cycle of the variability is quantified by the e-folding time scale of the annular mode autocorrelation function. Models vaguely capture the qualitative features of the Northern and Southern Annular Modes: Northern Hemisphere time scales are shorter than those of the Southern Hemisphere and peak in boreal winter, while Southern Hemisphere time scales peak in austral spring and summer. Models, however, systematically overestimate the time scales, particularly in the Southern Hemisphere summer, where the multimodel ensemble average is twice that of reanalyses. Fluctuation-dissipation theory suggests that long time scales in models could be associated with increased sensitivity to anthropogenic forcing. Comparison of model pairs with similar forcings but different annular mode time scales provides a hint of a fluctuation-dissipation relationship.

**Citation:** Gerber, E. P., L. M. Polvani, and D. Ancukiewicz (2008), Annular mode time scales in the Intergovernmental Panel on Climate Change Fourth Assessment Report models, *Geophys. Res. Lett.*, 35, L22707, doi:10.1029/2008GL035712.

### 1. Introduction

[2] The Northern and Southern Annular Modes (NAM and SAM) are the dominant patterns of variability in the extratropics on intraseasonal to interdecadal time scales [Thompson and Wallace, 2000]. The patterns characterize a meridional vacillation of the midlatitude, eddy driven jets in the Northern and Southern Hemispheres (NH and SH), respectively. A significant component of recent and future climate change consists of a poleward shift of the jets (and correspondingly, the storm tracks) and this shift projects strongly on the annular mode patterns [e.g., Yin, 2005; Miller et al., 2006; Son et al., 2008b]. Given the widespread use of annular modes as indicators of climate change, it is important to assess the ability of models in the Intergov-

ernmental Panel on Climate Change Fourth Assessment Report (IPCC AR4) to correctly simulate them.

[3] The annular modes characterize both spatial and temporal variability of the jet stream. Several studies have shown that their *spatial* structure is quite generic, and largely a consequence of the conservation of angular momentum and the mean structure of the midlatitude jets [e.g., Gerber and Vallis, 2005; Wittman et al., 2005]. The *temporal* structure of the annular modes, however, is more dynamically complex, potentially involving eddy-mean flow feedback [e.g., Robinson, 1996, 2006; Lorenz and Hartmann, 2001, 2003; Gerber and Vallis, 2007; Son et al., 2008a], synoptic wave breaking and high latitude blocking [e.g., Benedict et al., 2004; Woollings et al., 2008; Strong and Magnusdottir, 2008] and interaction between the troposphere and stratosphere [e.g., Baldwin et al., 2003; Wittman et al., 2004; Gerber and Polvani, 2008].

[4] Baldwin et al. [2003] characterize the temporal structure of the annular modes by computing, as a function of season and height, the e-folding time scale of the annular mode index autocorrelation function. This time scale, hereafter referred to as the “AM time scale”  $\tau(t, p)$ , quantifies the persistence of midlatitude jet anomalies, providing an integrated measure of variability on both intraseasonal and interannual frequencies. The seasonal structure of the AM time scale differs between the two hemisphere in a surprising way: the NAM time scale peaks during the boreal winter, while the SAM time scale peaks in the austral spring and summer. A stringent test of a model’s ability to capture the annular modes, then, is to correctly simulate their observed temporal variability. In this paper we assess the IPCC AR4 models by comparing their AM time scales to those in reanalysis observations.

### 2. Data and Methods

[5] Daily reanalyses of zonal wind from 1961–2000 were obtained from the National Centers for Environmental Prediction-National Center for Atmospheric Research (NCEP-NCAR) data set. Reanalyses of the Southern Hemisphere before 1979 were not used, due to the scarcity of observations in this period. Daily zonal wind output was obtained for 17 models in the World Climate Research Programme’s (WCRP’s) Coupled Model Intercomparison Project phase 3 (CMIP3) multimodel data set, as listed in Table 1. We used data from all models listed by Meehl et al. [2007] that archived daily zonal winds. For each model, a total of 120 years of winds were used from three integrations: the preindustrial control (40 years), the 20C3M simulation of 20th century climate (1961–2000), and the A1B scenario (2046–2065 and 2081–2100). In cases where modeling groups provided ensembles with multiple integra-

<sup>1</sup>Department of Applied Physics and Applied Mathematics, Columbia University, New York, New York, USA.

<sup>2</sup>Now at Courant Institute of Mathematical Sciences, New York University, New York, New York, USA.

<sup>3</sup>Department of Applied Physics and Applied Mathematics and Department of Earth and Environmental Science, Columbia University, New York, New York, USA.

<sup>4</sup>Program in Applied Physics, Fu Foundation School of Engineering and Applied Science, Columbia University, New York, New York, USA.

**Table 1.** CMIP3 Model Output Used in This Study<sup>a</sup>

Model	PIC	20C3M	A1B
BCCR-BCM2.0	1	1 <sup>b</sup>	1
CGCM3.1 (T47)	1	5	3
CGCM3.1 (T63)	1	1	1
CNMR-CM3	1	1	1
CSIRO-Mk3.0	1	2	1
ECHAM5/MPI-OM	1 <sup>c</sup>	2	2
FGOALS-g1.0	1	3	3
GFDL-CM2.0	1	1	1
GFDL-CM2.1	1	1	1
GISS-AOM	1	1	1
GISS-EH	1	1	0 <sup>d</sup>
GISS-ER	1	1	1
INM-CM3.0	1	1	1
IPSL-CM4	1	2	1
MIROC3.2 (hires)	1	1	1
MIROC3.2 (medres)	1	1	1
MRI-CGCM2.3.2	1	1	1

<sup>a</sup>‘PIC’ refers to the preindustrial control experiment, and the number in each cell shows the number of ensemble runs available. Details of the models are discussed by *Meehl et al.* [2007].

<sup>b</sup>Only 38 years from this integration are available.

<sup>c</sup>We use 1860–1899 from a 20C3M integration.

<sup>d</sup>The A1B scenario is not available.

tions, we computed the time scales independently for each ensemble member, and then averaged the results together. Each model, however, was given equal weight in the multimodel ensemble averages.

[6] The NAM and SAM were defined independently at each pressure level as the first Empirical Orthogonal Function (EOF) of the daily, deseasonalized, latitude weighted, zonal mean geopotential height poleward of 20° in each hemisphere, respectively. Because daily geopotential height was not archived for models, the anomalous zonal mean geopotential height  $\bar{Z}_{bal}$  was reconstructed from the zonal mean zonal wind  $\bar{u}$  at each pressure level and day, independently, by assuming geostrophic balance:

$$\bar{Z}(\phi)_{bal} = -r_0 g^{-1} \int_{-\pi/2}^{\phi} f \bar{u} d\phi + c, \quad (1)$$

where  $r_0$ ,  $g$ , and  $f$  are the radius of the earth, gravitational acceleration, and Coriolis parameter, respectively, and the integration constant  $c$  was chosen such that  $\int_{-\pi/2}^{\pi/2} \bar{Z}_{bal} r_0 \cos\phi d\phi = 0$ , thus ensuring conservation of mass. Data was deseasonalized by subtracting the annual cycle (computed by averaging all 40, or 20, years in each integration segment, separately) smoothed by a 31 day running mean from each year. For computing the annual cycle, the 121st day, Apr 30, was removed from leap years. A  $\sqrt{\cos\phi}$  latitude weighting accounts for the bias due to the shrinking latitude circle [*North et al.*, 1982]. The ‘‘annular mode index’’ was defined as the Principal Component time series associated with the first EOF and deseasonalized. The autocorrelation function of the index and its e-folding time scale were then computed exactly as in the work by *Baldwin*

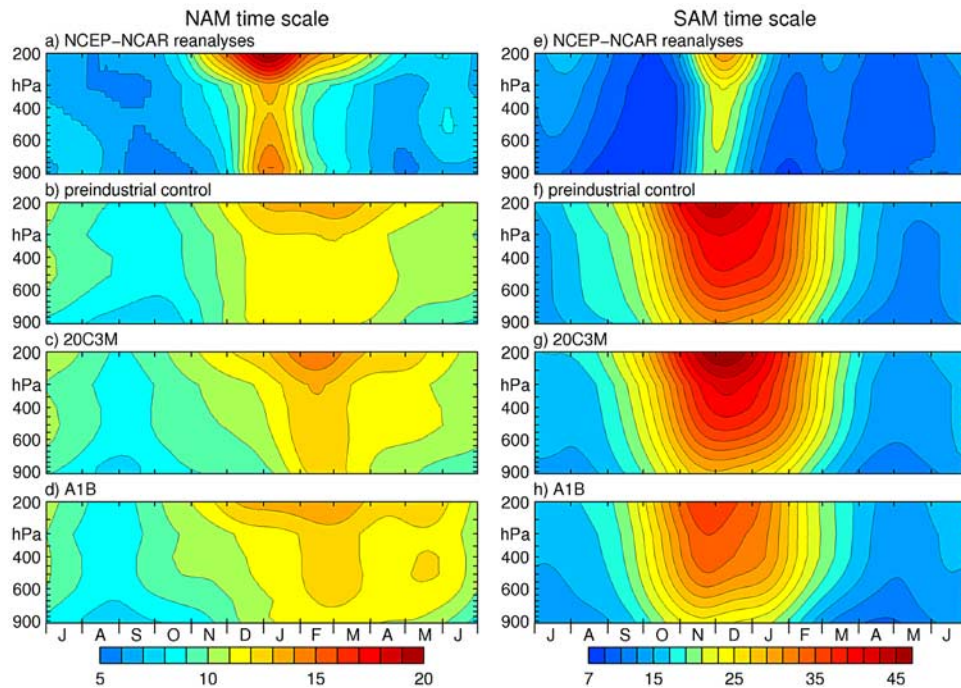


**Figure 1.** The annular mode time scale  $\tau$  (in days) based on the reconstructed zonal mean geopotential height, as a function of season and height. (a and e) NAM and SAM time scales computed from NCEP-NCAR reanalyses. (b, c, d, f, g, and h) Multimodel ensemble average time scales for the two hemispheres based on the preindustrial control, 20C3M, and A1B integrations. Figures 1c and 1g are most directly comparable to the reanalyses, as they are based on the same years (1961–2000) in the 20C3M integration as the reanalyses, but the similarity of the bottom three plots on each side suggests that the annular structure of  $\tau$  is insensitive to long term trends in the forcing. The slight reduction in SAM time scales in the A1B scenario, Figure 1h, is in part due to the absence of GISS-EH model data for this integration, and may also be influenced by use of two 20 year (not one 40 year) segments.

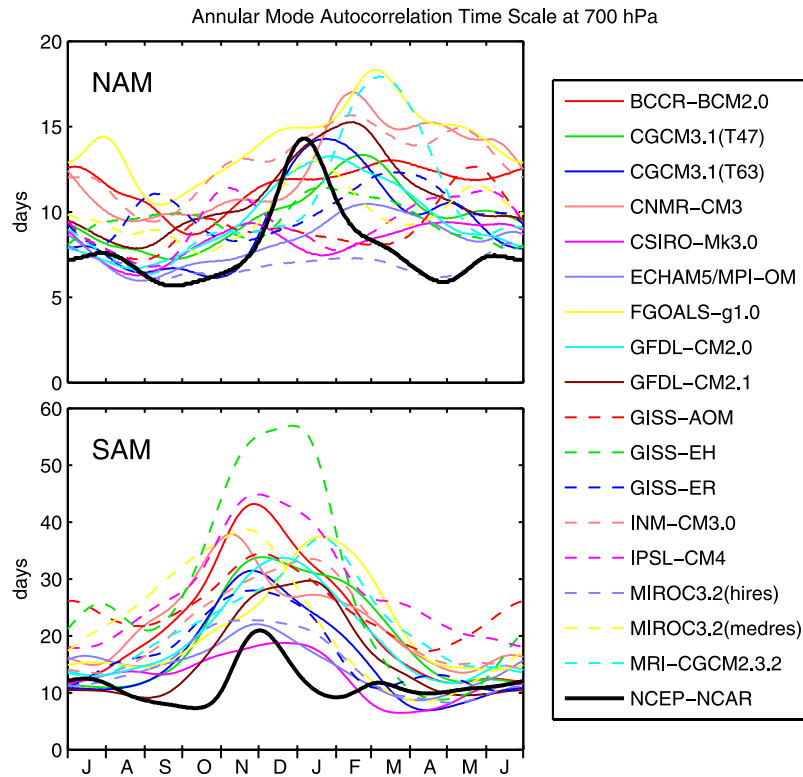


**Figure 2.** Individual model and reanalyses profiles of the AM time scale  $\tau$  as a function of season at 700 hPa, for the (top) Northern and (bottom) Southern Hemispheres. For each model,  $\tau$  values computed from all preindustrial control, 20C3M, and A1B integration ensemble members were averaged together to produce one profile per model. As discussed by Gerber *et al.* [2008], the uncertainty of  $\tau$  is a function of  $\tau$  itself. We estimate the uncertainty in each individual model's  $\tau$  (as quantified by its standard deviation) to be between 2 and 4 days in the NH and 3 and 9 days in the SH, with greater uncertainties being associated with longer time scales.

*et al.* [2003]. For fluctuation dissipation computations, a two-dimensional EOF of the daily zonal mean zonal wind as a function of latitude and pressure was computed, as in the work by Gerber *et al.* [2008].

### 3. Results

[7] Annular modes are traditionally defined from geopotential height fields, but models in the CMIP3 data set did not archive daily geopotential height as function of pressure. Hence we modified the analysis of Baldwin *et al.* [2003] to use the zonal wind, which was archived with daily values. We first validate the use of our alternative computation of the annular mode. In reanalyses, annular mode indices based on  $\overline{Z_{bal}}$  correlate extremely highly with indices based on the actual zonal mean geopotential height  $\overline{Z}$  (average correlation 0.990/0.996 in the NH/SH, respectively) and very highly with EOFs of the 2D geopotential height  $Z$  (average correlation 0.811/0.956 for NH/SH) through the depth of the troposphere.

[8] Figures 1a and 1e illustrate the AM time scale computed from the reconstructed zonal mean geopotential height  $\overline{Z_{bal}}$  from NCEP-NCAR reanalyses in the NH and SH, respectively. Comparison with Baldwin *et al.* [2003, Figure 1] reveals that the AM time scales computed from  $\overline{Z_{bal}}$  exhibit the same key features as those computed from the two dimensional geopotential height. Thus our method

preserves the seasonal and vertical structure found by the original procedure.

[9] Having established an observational benchmark from the reanalyses, we turn to the AM time scales in the IPCC AR4 models. Panels (b,f), (c,g), and (d,h) of Figure 1 show the multimodel ensemble mean NAM and SAM time scale  $\tau$ , as a function of season and height, from three CMIP3 data set experiments: the preindustrial control, 20C3M, and A1B scenarios, respectively. First, we find that the ensemble average AM time scales are nearly the same in all three experiments. This suggests that multimodel ensemble average time scale is robust, and that 20th and 21st century trends do not significantly impact the AM time scales. Second, we find that the time scales are considerably longer in models than in reanalyses, particularly in the Southern Hemisphere. Third, we find that the models capture the key NAM vs. SAM differences: AM time scales in the NH are shorter than those in the SH and peak in the boreal winter, while time scales in the SH reach their maximum in the austral spring and summer. Lastly, we find that the IPCC AR4 models vaguely capture the observed vertical structure.

[10] The ensemble average seasonal cycle in the AM time scale  $\tau$ , however, is much broader in the models than in the reanalyses. Also, the peak is delayed by approximately a month in the Northern Hemisphere. The broadening of the annual cycle might reflect phase differences between the models, but individual models generally exhibit broader peaks, as illustrated in Figure 2. Notably, the SAM time



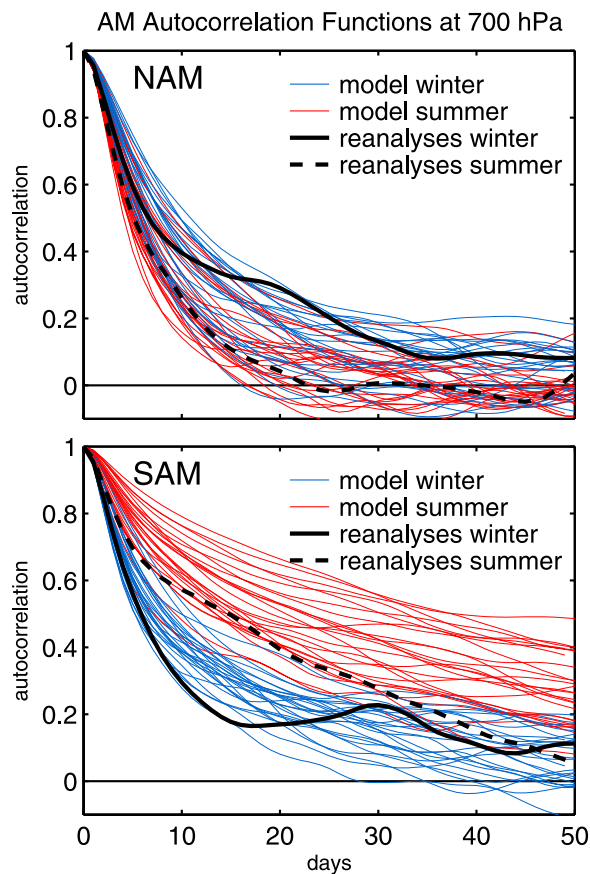


**Figure 3.** The autocorrelation functions of the annular mode at 700 hPa from the reanalyses (thick black contours) and the model 20C3M scenario integrations (thin colored contours). In the NAM plot, boreal winter autocorrelation functions are for January 15, and summer plots for August 15. In the Southern Hemisphere, austral winter plots are for June 1, and summer plots for December 1. These dates are chosen to best capture the extremes in both reanalyses and models. The AM autocorrelation functions of the preindustrial control and A1B scenario integrations (not shown) are similar to those of the 20C3M shown here.

scale  $\tau$  computed for each model individually is broader and longer than that in reanalyses for *every single model* during the austral summer. Also, individual models do not robustly capture the seasonal cycle of the NAM; some models exhibit multiple peaks, others none at all.

[11] To demonstrate that these qualitative results are robust, i.e., independent of the specific procedure used to quantify the persistence by  $\tau$ , we show actual samples of the AM autocorrelation functions at 700 hPa in Figure 3. The models grossly capture the reversed seasonal cycle in the two hemispheres, albeit less so in the NH, and generally overestimate the persistence of the AM.

[12] This overestimation might have implications for the models' sensitivity to anthropogenic forcing. If a fluctuation-dissipation relationship exists in the models [Leith, 1975; Ring and Plumb, 2008], trends in the annular modes (corresponding to shifts in the jets) might be larger in models with longer AM time scales, as illustrated by Gerber *et al.* [2008]. For the IPCC AR4 scenario integrations, such

a comparison is complicated by the fact that different models used different physical forcings (e.g., ozone) and exhibit different climate sensitivities. As a consequence, a clear relationship between  $\tau$  and the AM trends across all models could not be identified. Differences in parameterizations and forcings, however, can be minimized by comparing two sets of model results submitted by the same modeling group, but run at different numeric resolution, as was done with the CGCM3.1 and MIROC3.2 models.

[13] Gerber *et al.* [2008] found that the AM time scales in a GCM with simplified physics decrease as the horizontal resolution is increased. This is also the case with CGCM3.1 and MIROC3.2, as seen in the second column of Table 2. Here we focus on the SAM time scales and trends in NDJ, where differences between the models are most extreme. The higher resolution versions of each model exhibit shorter timescales than the lower resolution versions, and are thus closer to reanalysis observations. The third and fourth columns show the annular mode response to anthropogenic forcing in the A1B scenario, as quantified by the trend in the SAM over two different periods. In both models, the high resolution versions with *shorter AM time scales* exhibit *weaker AM trends* in the A1B scenario forcing, as one would expect from fluctuation-dissipation theory. Results from just two models are clearly not sufficient to make definitive claims. They suggest, however, that a fluctuation-dissipation relationship might be present in the IPCC AR4 models, and this merits future experiments with a more clearly defined forcing across multiple models.

#### 4. Discussion and Conclusions

[14] We have assessed the temporal structure of the annular modes in 17 IPCC AR4 coupled climate models by comparing their annular mode time scales as a function of pressure and season with those found in NCEP-NCAR reanalyses. We find that the models capture the gross features of the temporal structure of the NAM and SAM and the key inter-hemispheric differences. The models, however, systematically overestimate the time scales, particularly in the SH spring and summer, and exhibit much broader annual cycles in both hemispheres, particularly in the NH, where the annual cycle is only robust in the

**Table 2.** Evidence of a Possible Fluctuation-Dissipation Relationship in CGCM3.1 and MIROC3.2<sup>a</sup>

Model	$\tau$ (days)	SAM Trend	
		1980–2055	1980–2090
CGCM3.1 (T47)	32	0.71	0.76
CGCM3.1 (T63)	26	0.58	0.61
MIROC3.2 (medres)	35	0.94	0.67
MIROC3.2 (hires)	22	0.30	0.43

<sup>a</sup>The second column shows the SAM time scale  $\tau$  and the third and fourth columns the response of the annular mode, as quantified by the trend in the SAM index between 1980–2055 and 1980–2090, respectively. Values are based on 2-D latitude-pressure EOFs of the tropospheric zonal mean zonal wind to provide a measure of the vertically weighted circulation and are averaged for months NDJ. The trend is computed by projecting the difference in the climatological winds between 1960–2000 and 2046–2065 or 2081–2100 on to the annular mode pattern; positive values indicate poleward expansion of the jet stream. The trends are scaled relative to the variance of the annular mode in each model and so have units of standard deviations per century.

multimodel ensemble mean and the time of peak time scales is delayed by over a month relative to reanalyses.

[15] We note that the key differences between the NAM and SAM time scales are far from fully explained. Studies with idealized GCMs suggest that topography reduces the AM time scales by limiting eddy-mean flow feedback [Gerber and Vallis, 2007; Son et al., 2008a], and this could explain the longer time scales of the SAM relative to the NAM. The source of the 2 month offset (as opposed to 6) in the annual cycle of the NAM and SAM is less well understood. The results of Baldwin et al. [2003] suggest that the stratosphere may play a role in increasing the NAM time scale during the boreal winter and the SAM time scale during the austral spring and summer. However, since the IPCC AR4 models generally do not fully resolve the stratosphere and its variability (e.g., sudden warming events), the origin of the seasonal cycle may not depend critically on the details of the stratospheric circulation. The stratosphere, nonetheless, may be important for sharpening the seasonal cycle.

[16] Comparison of identical models integrated at different resolutions, as done by two modeling groups, suggests that increased resolution may reduce the positive bias in AM time scales relative to reanalyses. Associated with the reduction time scale is a reduced sensitivity of the annular mode to anthropogenic forcing, consistent with fluctuation dissipation theory. Potential for a fluctuation-dissipation relationship in the atmosphere-ocean system suggests that accurate simulation of the annular modes and other internal modes of variability may be important for accurate simulation of climate change. In any case, correct representation of the temporal structure of the annular modes has large implications for the regional climate in the IPCC AR4 models, particularly in mid and high latitudes. Atmospheric moisture and other tracer transports, interaction between the atmosphere and ocean, sea ice extent, and aspects of the global carbon cycle depend critically on the location and persistence of the midlatitude westerlies.

[17] **Acknowledgments.** We thank Judith Perlwitz and an anonymous reviewer for instructive comments, Mark Baldwin for suggesting the procedure to reconstruct the geopotential height from the zonal wind, the IPCC AR4 modeling groups, the Program for Climate Model Diagnosis and Intercomparison, the WCRP's Working Group on Coupled Modeling, the Office of Science of the U.S. Department of Energy, and the National Oceanic and Atmospheric Administration-Cooperative Institute for Research in Environmental Sciences Climate Diagnostics Center. This work was funded, in part, by a grant from the National Science Foundation to Columbia University.

## References

Baldwin, M. P., D. B. Stephenson, D. W. J. Thompson, T. J. Dunkerton, A. J. Charlton, and A. O'Neill (2003), Stratospheric memory and skill of extended-range weather forecasts, *Science*, *301*, 636–640.  
 Benedict, J. J., S. Lee, and S. B. Feldstein (2004), Synoptic view of the North Atlantic Oscillation, *J. Atmos. Sci.*, *61*, 121–144.

Gerber, E. P., and L. M. Polvani (2008), Stratosphere-troposphere coupling in a relatively simple AGCM: The importance of stratospheric variability, *J. Clim.*, in press.  
 Gerber, E. P., and G. K. Vallis (2005), A stochastic model for the spatial structure of annular patterns of variability and the NAO, *J. Clim.*, *18*, 2102–2118.  
 Gerber, E. P., and G. K. Vallis (2007), Eddy-zonal flow interactions and the persistence of the zonal index, *J. Atmos. Sci.*, *64*, 3296–3311.  
 Gerber, E. P., S. Voronin, and L. M. Polvani (2008), Testing the annular mode autocorrelation timescale in simple atmospheric general circulation models, *Mon. Weather Rev.*, *136*, 1523–1536.  
 Leith, C. E. (1975), Climate response and fluctuation dissipation, *J. Atmos. Sci.*, *32*, 2022–2026.  
 Lorenz, D. J., and D. L. Hartmann (2001), Eddy-zonal flow feedback in the Southern Hemisphere, *J. Atmos. Sci.*, *58*, 3312–3327.  
 Lorenz, D. J., and D. L. Hartmann (2003), Eddy-zonal flow feedback in the Northern Hemisphere winter, *J. Clim.*, *16*, 1212–1227.  
 Meehl, G. A., C. Covey, T. Delworth, M. Latif, B. McAvaney, J. F. B. Mitchell, R. J. Stouffer, and K. E. Taylor (2007), The WCRP CMIP3 multimodel dataset, *Bull. Am. Meteorol. Soc.*, *88*, 1383–1394.  
 Miller, R. L., G. A. Schmidt, and D. T. Shindell (2006), Forced annular variations in the 20th century Intergovernmental Panel on Climate Change Fourth Assessment Report models, *J. Geophys. Res.*, *111*, D18101, doi:10.1029/2005JD006323.  
 North, G. R., T. L. Bell, R. F. Cahalan, and F. J. Moeng (1982), Sampling errors in the estimation of empirical orthogonal functions, *Mon. Weather Rev.*, *110*, 699–706.  
 Ring, M. J., and R. A. Plumb (2008), The response of a simplified GCM to axisymmetric forcings: Applicability of the fluctuation-dissipation theorem, *J. Atmos. Sci.*, in press.  
 Robinson, W. A. (1996), Does eddy feedback sustain variability in the zonal index?, *J. Atmos. Sci.*, *53*, 3556–3569.  
 Robinson, W. A. (2006), On the self-maintenance of midlatitude jets, *J. Atmos. Sci.*, *63*, 2109–2122.  
 Son, S.-W., S. Lee, S. B. Feldstein, and J. E. TenHoeve (2008a), Time scale and feedback of zonal mean flow variability, *J. Atmos. Sci.*, *65*, 935–952.  
 Son, S.-W., et al. (2008b), The impact of stratospheric ozone recovery on the Southern Hemisphere westerly jet, *Science*, *320*, 1486–1489, doi:10.1126/science.1155939.  
 Strong, C., and G. Magnusdottir (2008), How Rossby wave breaking over the Pacific forces the North Atlantic Oscillation, *Geophys. Res. Lett.*, *35*, L10706, doi:10.1029/2008GL033578.  
 Thompson, D. W. J., and J. M. Wallace (2000), Annular modes in the extratropical circulation. Part I: Month-to-month variability, *J. Clim.*, *13*, 1000–1016.  
 Wittman, M. A. H., L. M. Polvani, R. K. Scott, and A. J. Charlton (2004), Stratospheric influence on baroclinic lifecycles and its connection to the Arctic Oscillation, *Geophys. Res. Lett.*, *31*, L16113, doi:10.1029/2004GL020503.  
 Wittman, M. A. H., A. J. Charlton, and L. M. Polvani (2005), On the meridional structure of annular modes, *J. Clim.*, *18*, 2119–2122.  
 Woollings, T. J., B. J. Hoskins, M. Blackburn, and P. Berrisford (2008), A new Rossby wave-breaking interpretation of the North Atlantic Oscillation, *J. Atmos. Sci.*, *65*, 609–626.  
 Yin, J. H. (2005), A consistent poleward shift of the storm tracks in simulations of 21st century climate, *Geophys. Res. Lett.*, *32*, L18701, doi:10.1029/2005GL023684.

D. Ancukiewicz, Program in Applied Physics, Fu Foundation School of Engineering and Applied Science, Columbia University, 510 S. W. Mudd Building, 500 West 120th Street, New York NY 10027, USA.

E. P. Gerber, Courant Institute of Mathematical Sciences, New York University, 251 Mercer Street, New York NY 10012, USA. (gerber@cims.nyu.edu)

L. M. Polvani, Department of Applied Physics and Applied Mathematics, Columbia University, 200 S. W. Mudd Building, MC 4701, 500 West 120th Street, New York NY 10027, USA.